DOI: 10.61782/fa.2023.0886

forum acusticum 2023

NONLINEAR FACTORS IN SINGLE AND DOUBLE BACKPLATE CAPACITIVE TRANSDUCERS

Georgios Printezis[*,1] **Niels Aage**[2] **Frieder Lucklum**[1]
Centre for Acoustic-Mechanical Microsystems,
[1]*Department of Electrical and Photonics Engineering,*
[2]*Department of Civil and Mechanical Engineering,*
Technical University of Denmark,
DK-2800 Kgs. Lyngby,
Denmark

ABSTRACT

Capacitive microphones are widely being used in many applications as high-precision instruments for measurement to audio capturing microelectromechanical (MEMS) sensors in common mobile devices, such as portable computers, mobile phones, and hearing aids. The latter have successfully replaced previous technologies such as the electret condenser microphones (ECM) due to their lower sensitivity to temperature variations, smaller footprint, and lower sensitivity to vibration, having a consistent frequency response. However, their widespread use has increased the demand for tighter specifications, especially in loud environments where the total harmonic distortion (THD) and the acoustic overload point (AOP) become significant parameters to the devices' performance. With the aim of providing a more detailed physical understanding of the nonlinear dynamical behavior of double backplate transducers a DC biased parallel plate model of such a device is developed and the effect of the nonlinear factors to the model's nonlinear response are discussed compared to the ones of a single backplate model.

Keywords: *Capacitive Microphones; Microelectromechanical (MEMS) Microphones; Dual-Backplate; Nonlinearities; Nondimensionalization; Nonlinear Factors*

**Corresponding author*: *giopri@outlook.com.*

1. INTRODUCTION

A microphone is an electroacoustic transducer that captures an acoustic signal and converts it into an electrical one with proportionate characteristics. A lot of progress has been done through the years in terms of modeling, designing, and characterizing such a device. Initially intended for the study and transmission of speech , microphones are now to be found in many every day devices like mobile phones, portable computers, smart speakers, and hearing aids.

Their shapes and sizes can vary as well as the physical way by which sound is converted to electricity; the *transduction principle*. Taking advantage of the advances made in silicon fabrication technology micro-electromechanical (MEMS) microphones are now being massively produced. The dominating transduction principle utilized in this type of sensors is the *capacitive*. MEMS microphones utilizing this principle have successfully replaced the previous technology in relevant applications, the electret condenser microphones (ECM), as they can have lower sensitivity to temperature variations, smaller footprint, and lower sensitivity to vibration, and a frequency response with low variability from part to part [1].

Their widespread use has lead to ever tightening specifications as the demand for higher performing products increases. High levels of acoustic signal from the audible to the ultrasonic range can have a negative affect to the overall electroacoustic response of the device. Ideally one would like the device to be responding *linearly* to acoustic input meaning that the response should be analogous to the latter. In reality though linearity is a property that can

only be approximated in a specific dynamic and frequency range for a given system.

A quantitative measure of the *nonlinear* response of the device is the *Total Harmonic Distortion* (THD) which is essentially a way to assess the importance of the response at integer multiples of the frequency of a pure harmonic tone (*harmonics*) at the input with respect to the response at that frequency (*fundamental*). The *Acoustic Overload Point* (AOP) is a more general measure that aims at characterizing the dynamic range of linearity. It is the point on which when the system is excited with a pure tone at a certain frequency (typically at 1 kHz) the calculated THD surpasses a certain threshold percentage (typically within the range of 1% to 10%).

In their most simple configuration, capacitive MEMS microphones incorporate the sensor element, along with its packaging and analog and possibly digital circuitry that afford signal conditioning, conversion, and read-out capability. The sensor element in many cases consists of a number of flexible and rigid electrodes charged and placed in such a manner so that an output signal can be obtained when an acoustic wave is impinging.

Sources of nonlinearities in these devices can originate from the coupled electromechanical motion of the diaphragm, the charging of the electrodes, or along the signal path through its circuitry. Previous work on some times also referred to as *true-differential* microphones [2–5] has been completely neglecting any nonlinearities related to the charging of the electrodes and either restrict the analysis to one possible output stage or completely disregard it. In this work we model such a microphone taking into account its charging as a source of nonlinearity as well as the output stage taking into consideration the parasitic capacitances.

In an effort to come up with practical physical indicators of nonlinearity at the sensor level we nondimensionalize the equations that describe the dynamic behavior of a lumped representation of the sensor together with its charging scheme. We calculate the THD for a number of different frequencies and compare the effect of those *factors* for two different configurations one with a flexible diaphragm opposite a perforated rigid backplate [1] and one with a flexible diaphragm between two perforated rigid backplates. The linear superiority of the *double* backplate sensor is evident in our results.

2. THE MODELS

In this section we briefly go through the lumped representation of the single and double backplate configurations.

2.1 Single backplate

In figure 1 a sketch of the single backplate sensor system representation is given. The mechanical and acoustical elements in the system are represented as mechanical components in the sketch and the biasing network that charges the transducer is connected in such a way so that for a relative displacement of the electrodes a fluctuating voltage output can be obtained across them in response.

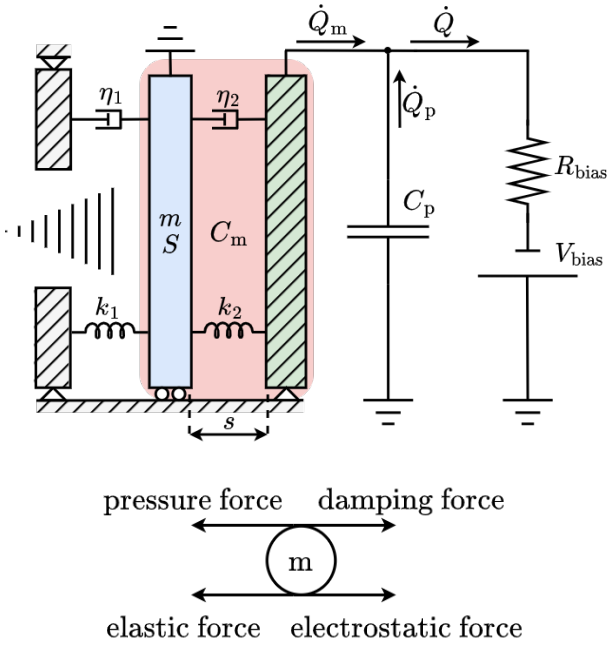

Figure 1: Electromechanical network sketch of a parallel plate capacitive transducer. Sound pressure is exerted on the electrodes through the inlet and *front-chamber* of the device. Elements are not drawn at scale. The circle with the adjacent arrows represents the point-mass of the moving electrode.

Figure 3 shows that the electrodes are charged using a resistor (R_bias) in series with the electrodes and the DC bias voltage (V_bias). A parasitic capacitance (C_p) is included in the model, which represents the capacitance of

the conductive elements in the transducer that do not respond to an impinging acoustic signal and the input capacitance of the following amplification stage [6]. This capacitance is connected in parallel to the electrodes. The moving electrode, which has a mass (m) and an area (S), is located a distance (s) away from the stationary electrode of the same area, and together they form the variable capacitance (C_m). The displacement of the moving electrode is damped mostly due to energy dissipation caused by air movement between the electrodes and through the backplate holes, with a viscous damping coefficient (η_2), as well as radiation of air with a viscous damping coefficient (η_1). Elastic forces on the moving electrode come from the air in the back chamber of the transducer, with a mechanical stiffness (k_2), and from its mechanical support, with a mechanical stiffness (k_1).

Figure 2 shows the proposed circuit equivalent linear system that models the mechanical force acting on the moving electrode using the impedance analogy. The mass and compliance of the volume of air between the electrodes are omitted from the model, assuming that the number and rate of the perforations are sufficiently large. Since the membrane's movement is modeled for a rigid backplate, the velocity (v) induced by the pressure force (F_p) that flows through all the mechanical components is the same and therefore placed in series. The mechanical radiation resistance is represented by R_rad, while L_rad is the mass of the radiating air. The compliance of the moving electrode is represented by C_d, which is equal to C'_d/ν, where C'_d is the compliance due to the mechanical support of the moving electrode and ν is the spring softening factor [7]. The mass of the moving electrode is represented by L_d. The mechanical resistance caused by air streaming through slits and holes in the narrow air gap between the diaphragm and the backplate is represented by R_gap, and L_gap is the respective air mass that is considered negligible in the calculations. The compliance of the volume of air enclosed in the back chamber of the device is represented by C_bc. It's important to note that C_d should not be confused with C_m, which represents the instantaneous electrical capacitance formed by the electrodes. Finally, the model assumes that the backplate is not compliant.

2.2 Double backplate

In figure 4 a sketch of the double backplate sensor system representation is given. In this case as well the mechanical and acoustical elements in the system are represented as mechanical components and the biasing network that

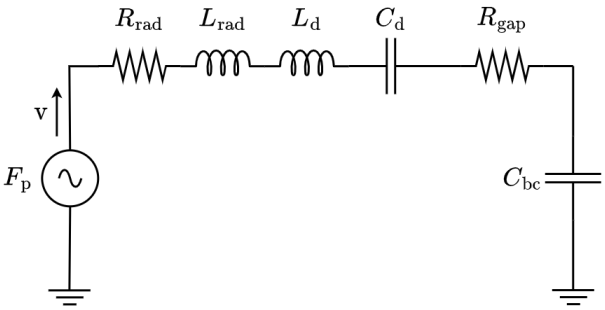

Figure 2: Pressure force equivalent circuit of a parallel plate capacitive transducer.

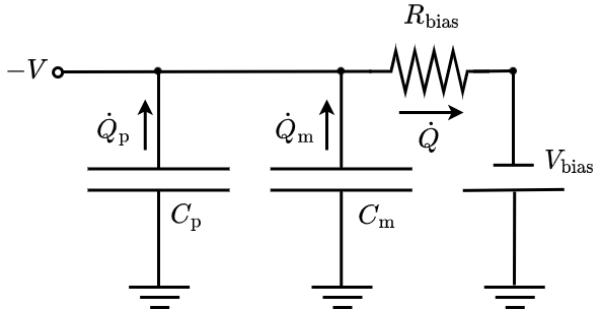

Figure 3: Electrical charging circuit of a parallel plate capacitive transducer.

charges the transducer is connected in such a way so that for a relative displacement of the electrodes a fluctuating voltage output can be obtained across them in response.

The electrodes once more charged using a resistor (R_bias) which is shared among the capacitances formed by the electrodes that represent the backplates and the moving electrode, with thickness h_d that represents the flexible diaphragm, as in figure 6. The bias voltage is applied to each capacitance so that a displacement of the moving electrode can create a voltage fluctuation to the output.

The model includes a parasitic capacitance (C_p) that can be formed by the conductive elements in an actual transducer that do not respond to an impinging acoustic signal as well as the input capacitance of the following amplification stage and is placed in parallel to the voltage output. The moving electrode that has a mass (m) and area (S) is at distances s_1 and s_2 from each of the stationary electrodes and form the variable capacitances $C_{\mathrm{m},1}$ and $C_{\mathrm{m},2}$ respectively. The damping in the displacement

of the moving electrode is assumed to be mostly related to the energy dissipation due to the air movement between the electrodes and through the backplate holes and due to radiation of air with viscous damping coefficient, represented in the figure as viscous damping η_1 and η_2. The elastic forces acting on the moving electrode are due to the air in the backchamber of the transducer with mechanical stiffness and its mechanical support represented in the figure as viscous damping k_1 and k_2.

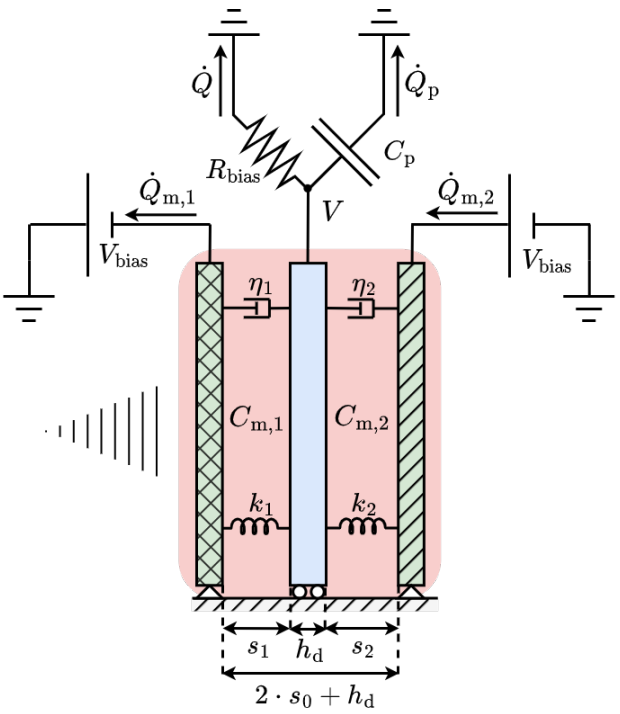

Figure 4: Electromechanical network sketch of a double backplate capacitive transducer.

Figure 5 represents the proposed circuit equivalent linear system in the impedance analogy of the mechanical force acting on the moving electrode. We omit the mass and compliance of the volume of air between the electrodes assuming that the number and rate of the perforations is large enough. Since we model the movement of the membrane for a rigid backplate the velocity (v) induced by the pressure force (F_p) that, as is the case for the single backplate model, flows through all the mechanical components is the same and thus are placed in series. R_rad is the mechanical radiation resistance. L_rad is the mass of the radiating air. C_d is the compliance of the moving electrode, due to the mechanical support of the moving electrode. L_d is the mass of the moving electrode. R_gap is the mechanical resistance caused by air streaming through slits and holes in the narrow air gap between the diaphragm and the backplate. C_bc is the compliance of the volume of air enclosed in the backchamber of the device. Finally, we assume that the backplates are not mechanically compliant.

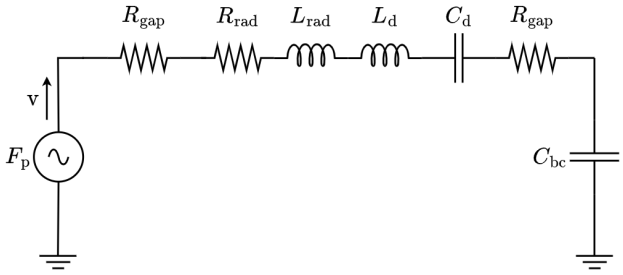

Figure 5: Pressure force equivalent circuit of a double backplate capacitive transducer.

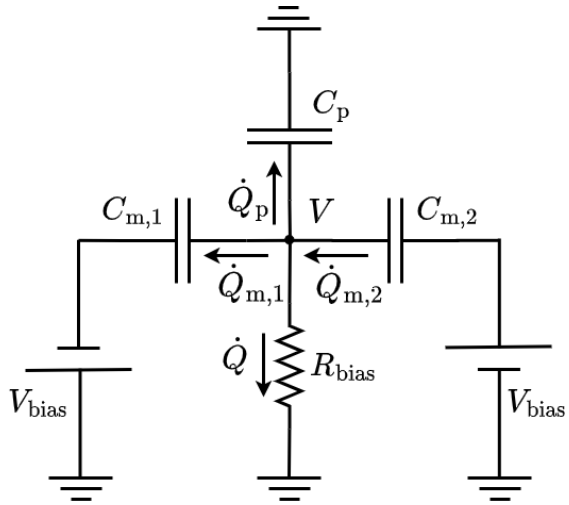

Figure 6: Electrical charging circuit of a double backplate capacitive transducer.

3. NONLINEAR FACTORS

Bellow the nondimensional nonlinear factors to the dynamical system's response are given. For a more detailed description and derivation for the single backplate configuration the reader is referred to [7]:

$$\lambda = \frac{1}{2} \cdot \frac{C_0 \cdot V_{\text{bias}}^2}{k \cdot s_0^2}, \tag{1}$$

which is related to the nonlinearities due to the *softening* of the elastic force and couples the charging to the mechanical behavior of the moving electrode,

$$c_{\text{p}} = \frac{C_{\text{p}}}{C_0}, \tag{2}$$

which is related to the uneven distribution of charge to the electrodes and the parasitics,

$$\sigma = \frac{\theta}{1+\theta}, \tag{3}$$

which acts as a factor to the nonlinear thin-film damping,

$$\tau_0 = \omega_{\text{n}} \cdot R_{\text{bias}} \cdot C_0, \tag{4}$$

which acts as damping to the fluctuation of the total charge stored in the transducer,

$$\rho_0 = \frac{p_0 \cdot S}{k \cdot s_0} \tag{5}$$

which is essentially the nondimensional impinging pressure force amplitude, and

$$\Omega = \frac{\omega}{\omega_{\text{n}}}, \tag{6}$$

which is the nondimensional excitation frequency when the system is harmonically excited with a single tone.
In the preceding equations,

$$C_0 = \frac{\varepsilon \cdot S}{s_0}$$

where ε is the dielectric permittivity of air, and s_0 the distance of the moving and the stationary electrodes at equilibrium in the absence of the electrostatic force, ω_{n} is the natural frequency of the mass-spring system, N and S_{h} are the number and cross-sectional area of each of the perforations in the backplate respectively,

$$\theta = 8 \cdot \frac{G(A)}{N}.$$

where

$$G(A) = \frac{A}{2} - \frac{A^2}{8} - \frac{\ln A}{4} - \frac{3}{8},$$

and k is the mechanical stiffness of the diaphragm due to its mechanical support.

4. RESULTS

In this section we compare the precedingly described transducer configuraions in terms of their nonlinear response to harmonic excitation at 1kHz. We use the parameters of the fitted single backplate model to measurements of microelectromechanical (MEMS) transducers and compare the nonlinear response of the two models for a number of excitation levels.

In figure 7 we present the pressure response of the two configurations for the first three harmonics, i.e. the fundamental, the 2$^{\text{nd}}$, and 3$^{\text{rd}}$ harmonic. A voltage follower amplification stage is assumed. A nearly complete suppression of the 2$^{\text{nd}}$ harmonic response can be observed for all excitation levels in the double backplate configuration. Not only that but the third harmonic is considerably suppressed compared to the single backplate configuration.

To prevent the output signal of the transducer from being affected by the load impedance an amplifying stage that acts as an impedance converter is necessary. If the transducer was to be directly connected to the load impedance of the next stage in the signal chain the readout could be severely and undesirably affected. To mitigate such an issue an amplifying stage that acts as an impedance converter is necessary. Depending on the readout quantity from the transducer a charge amplifier or voltage amplifier can be used [7]. To take into account the readout we assume the output stage to be linear and compare the total harmonic distortion for a voltage amplifier (THD_{V}) and a charge amplifier (THD_{Q}).

In figure 8 we present the time-domain response of the two configurations in a single period when the system is excited with 135 dB SPL. There we observe that the voltage response of the double backplate configuration is more symmetrical to the response of the single backplate. Nonetheless, the response still appears to be distorted. When excited with π phase difference the same asymmetry can be observed but this time the magnitude of the second half-cycle becomes larger. This can be attributed to the nonlinear thin film damping. Exciting initially the system from equilibrium the moving electrode accelerates moving away or towards a backplate. The velocity reaches its maximum value at equilibrium distance as the moving electrode accelerates towards the opposite direction inducing a high damping force. Returning to equilibrium in the final quarter-cycle the magnitude of the velocity is less than that in the second causing a deeper displacement towards the initial direction, and leading to the depicted voltage response.

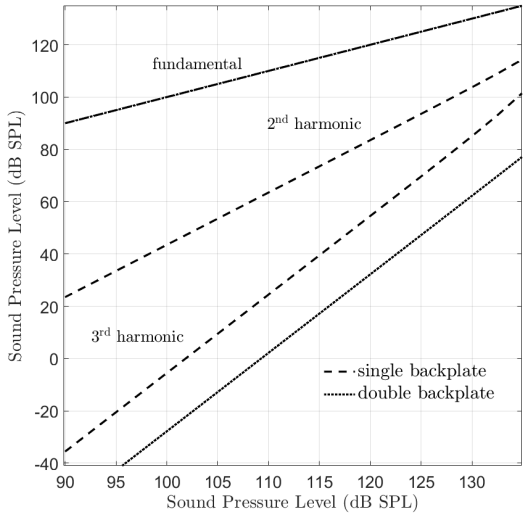

Figure 7: Pressure response of the single and double backplate models (*y-axis*) with respect to the impinging pressure level (*x-axis*) at 1 kHz. The fundamental coincides for both single and double backplate configurations.

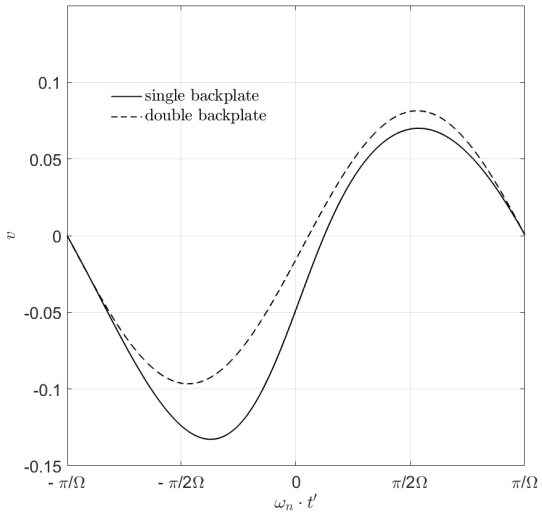

Figure 8: Voltage response of the single and double backplate models in a period when excited at 1 kHz with 135 dB SPL. $\Omega = \omega/\omega_{\mathrm{n}}$, where ω is the excitation frequency and ω_{n} is the natural frequency of the mass-spring system. t' (s) is the dimensional time variable.

In figure 9 we calculate the total harmonic distortion for both configurations assuming a voltage following and a charge amplification stage respectively. There we can observe that in both occasions the double backplate configuration is far more linear in its voltage response exhibiting very low harmonic distortion for the highest excitation levels.

To evaluate the importance of the different factors to the nonlinear voltage response of the transducer we propose the following two dimensional vector function with each element of the vector representing a metric associated with the amplification stage,

$$\boldsymbol{G}_x = \mathrm{diag}(\Delta \boldsymbol{THD})^{-1} \cdot \Delta_x \boldsymbol{THD} \qquad (7)$$

where

$$\boldsymbol{THD} = \begin{pmatrix} THD_{\mathrm{V}} \\ THD_{\mathrm{Q}} \end{pmatrix}.$$

In the preceding equation x is one of the nonlinear factors $(\lambda, c_{\mathrm{p}}, \sigma, \tau_0, \rho_0, \Omega)$, Δ_x symbolizes the change in $\boldsymbol{THD}$ for a very small change to the the corresponding nonlinear factor, and Δ symbolizes the change in $\boldsymbol{THD}$ for a very small change to all of the nonlinear factors. The metrics can be seen as the relative local derivative-based sensitivities of the nonlinear voltage response of such a transducer.

Using the nonlinear factors from [7] we observed that $\min(\boldsymbol{G}_\sigma) > .97$, indicating that for such a transducer the factor that mostly affects the nonlinear voltage response is σ which relates to the nonlinear thin-film damping.

5. CONCLUSION

In this paper we went into describing two configuration for MEMS microphones' sensors consisting of one and two backplates taking into account their charging through a biasing network with DC voltage and a resistor. We compared the voltage response of the single and double backplate configurations for the same nonlinear factors relating to the geometrical and biasing characterstics. Our results show that the configuration of the sensor having two backplates can be much more linear in its voltage response when compared with the single backplate case. By using a proposed metric we showed that the nonlinear damping due to the thin-film of air between the electrodes

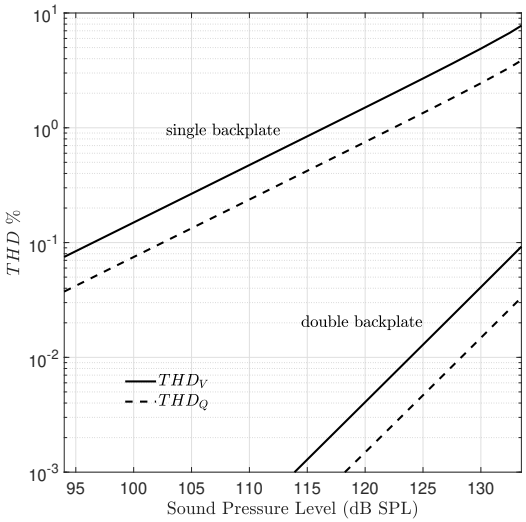

Figure 9: Total harmonic distortion (THD) calculated for the single and double backplate configurations.

contributes significantly to the nonlinear voltage response of such a transducer.

6. REFERENCES

[1] A. Khenkin, "Recommendations for mounting and connecting analog devices, inc.,bottom-ported mems microphones," tech. rep., ANALOG DEVICES, 2010.

[2] N. N. Peña-García, L. A. Aguilera-Cortés, M. A. González-Palacios, J.-P. Raskin, and A. L. Herrera-May, "Design and modeling of a MEMS dual-backplate capacitive microphone with spring-supported diaphragm for mobile device applications," *Sensors*, vol. 18, p. 3545, oct 2018.

[3] J. Liu, D. T. Martin, K. Kadirvel, T. Nishida, L. Cattafesta, M. Sheplak, and B. P. Mann, "Nonlinear model and system identification of a capacitive dual-backplate MEMS microphone," *Journal of Sound and Vibration*, vol. 309, pp. 276–292, jan 2008.

[4] J. Liu, D. T. Martin, T. Nishida, L. N. Cattafesta, M. Sheplak, and B. P. Mann, "Harmonic balance nonlinear identification of a capacitive dual-backplate MEMS microphone," *Journal of Microelectromechanical Systems*, vol. 17, pp. 698–708, jun 2008.

[5] D. T. Martin, J. Liu, K. Kadirvel, R. M. Fox, M. Sheplak, and T. Nishida, "A micromachined dual-backplate capacitive microphone for aeroacoustic measurements," *Journal of Microelectromechanical Systems*, vol. 16, pp. 1289–1302, dec 2007.

[6] S. Shubham and M. Nawaz, "Estimating parasitic capacitances in mems microphones using finite element modeling," *Excerpt from the Proceedings of the 2019 COMSOL Conference in Boston*, 2019.

[7] G. Printezis, N. Aage, and F. Lucklum, "A non-dimensional time-domain lumped model for externally dc biased capacitive microphones with two electrodes," *Available at SSRN*, 2023.